Journal of Computer-Aided Molecular Design, 11 (1997) 581–588.
KLUWER/ESCOM

J-CAMD 413

Molecular modeling of the intestinal bile acid carrier: A comparative molecular field analysis study

Peter W. Swaan*, Francis C. Szoka Jr. and Svein Øie**

Department of Biopharmaceutical Sciences, University of California, P.O. Box 0446, San Francisco, CA 94143-0446, U.S.A.

Received 13 February 1997
Accepted 15 May 1997

Keywords: Bile acids; Structure–transport relationship; Carrier-mediated transport; CoMFA; 3D QSAR

Summary

A structure–binding activity relationship for the intestinal bile acid transporter has been developed using data from a series of bile acid analogs in a comparative molecular field analysis (CoMFA). The studied compounds consisted of a series of bile acid–peptide conjugates, with modifications at the 24 position of the cholic acid sterol nucleus, and compounds with slight modifications at the 3, 7, and 12 positions. For the CoMFA study, these compounds were divided into a training set and a test set, comprising 25 and 5 molecules, respectively. The best three-dimensional quantitative structure–activity relationship model found rationalizes the steric and electrostatic factors which modulate affinity to the bile acid carrier with a cross-validated, conventional and predictive r^2 of 0.63, 0.96, and 0.69, respectively, indicating a good predictive model for carrier affinity. Binding is facilitated by positioning an electronegative moiety at the 24–27 position, and also by steric bulk at the end of the side chain. The model suggests substitutions at positions 3, 7, 12, and 24 that could lead to new substrates with reasonable affinity for the carrier.

Introduction

Bile acids play a critical role in a multitude of biological processes such as digestion, secretion and the regulation of cholesterol metabolism [1]. They undergo enterohepatic recycling caused by two specific sodium-dependent, carrier-mediated absorption mechanisms in the intestine and the liver [2]. Most investigations have been concerned with the characterization of the kinetics of uptake and secretion processes for bile salts, whereas only few studies have been carried out to elucidate the basic molecular mechanism for bile salt transport. Photoaffinity labeling techniques have revealed a number of proteins of the brush-border [3], cytosolic [4], and basolateral membranes [5] involved in the transfer of bile acids across the rat ileal enterocyte. A putative transport protein involved in coupled Na^+-bile acid transfer across the ileal brush-border membrane had a molecular weight of 99 kDa [2,6].

Because the proteins involved in cellular uptake and transport of bile acids have not yet been isolated, their three-dimensional (3D) structures are not identified and, hence, little is known about the spatial requirements for binding to and transport of bile acids by the ileal bile acid carrier. Studies in rat ileum have suggested that the number of hydroxyl substituents on a bile acid plays an important role in uptake. Among the free bile acids, 3,7,12-trihydroxy bile acids are more efficiently taken up by enterocytes than the dihydroxy acids, and the latter more than the monohydroxy bile acids [7,8]. However, no single hydroxy group is essential for transport. Orientation of the hydroxyl groups (α or β configuration) is of less importance. Triketo bile acids, such as taurodehydrocholic acid, are devoid of all hydroxyl groups and show considerably less transport [8].

The ileal bile acid carrier exhibits a wide substrate specificity: it not only transports its natural substrates, conjugated and unconjugated bile acids, but it also has

*Present address: Division of Pharmaceutics and Pharmaceutical Chemistry, College of Pharmacy, The Ohio State University, Columbus, OH 43210-1291, U.S.A.
**To whom correspondence should be addressed.

TABLE 1
STRUCTURE AND ACTIVITIES OF BILE ACID DERIVATIVES

#	X	R_3	R_7	R_{12}	1/%inhibition	clogP	CMR
1	OH	OH	OH	OH	0.077	3.08	11.00
2	$CH_2CH_2SO_3H$	OH	OH	OH	0.10	1.53	13.17
3	DF[a]	OH	OH	OH	0.025	2.87	18.22
4	EA	OH	OH	OH	0.026	–0.36	15.92
5	EAA	OH	OH	OH	0.016	–0.61	17.72
6	EAAA	OH	OH	OH	0.0169	–0.87	19.51
7	EASA	OH	OH	OH	0.018	–1.73	19.67
8	***EAYA***[b]	OH	OH	OH	***0.015***	***–0.119***	***22.18***
9	EFSA	OH	OH	OH	0.0174	–0.31	22.18
10	***EASAA***	OH	OH	OH	***0.0168***	***–1.99***	***21.47***
11	EASASA	OH	OH	OH	0.0123	–5.40	23.99
12	***EASPSA***	OH	OH	OH	***0.0138***	***–1.98***	***24.74***
13	***OH***	OH	H	H	***0.0108***	***6.60***	***10.69***
14	CH_3	OH	OH	OH	0.022	2.80	11.46
15	OH	H	H	H	0.011	8.69	10.54
16	OH	H	OH	OH	0.143	4.51	10.85
17	OH	OH	H	OH	0.10	5.16	10.85
18	OH	OH	OH	H	0.10	4.51	10.85
19	OH	OH	H	H	0.010	6.60	10.69
20	***OH***	NH_2	OH	OH	***0.011***	***0.26***	***11.21***
21	OH	=O	OH	OH	0.013	2.02	10.88
22	OH	OCHO	OCHO	OCHO	0.016	3.93	12.50
23	OH	OH	OCHO	OCHO	0.018	3.43	12.00
24	Lys	OH	OH	OH	0.012	0.77	14.57
25	Lys-ε-*t*BOC	OH	OH	OH	0.055	3.16	17.37
26	ε-D-Lys	OH	OH	OH	0.012	1.31	14.60
27	D-Asp	OH	OH	OH	0.011	1.38	13.45
28	D-Ala	OH	OH	OH	0.05	2.02	12.79
29	D-Ala-Ala	OH	OH	OH	0.011	1.76	14.59
30	D-Asp-α-benzyl ester	OH	OH	OH	0.111	3.23	16.42

[a] All amino acids are the L-stereoisomers and have a terminal amide group, unless noted otherwise.
[b] Bold italic indicates those compounds used in the test set.

been reported to transport a number of peptides and drugs conjugated to bile acids [9,10,16,17]. This points out the potential of the ileal bile acid carrier for increasing the oral bioavailability of drugs and, thus, additional structural information would help to predict compounds that might bind to this transporter.

In this study, we carried out comparative molecular field analysis (CoMFA) [11], a 3D quantitative structure–activity relationships (3D QSAR) technique that has been applied previously with considerable success [12–14] and is able to give a predictive description of global structural requirements for interactions between substrates and receptors (transporters, in our case) using binding or activity data [15]. We describe results from a CoMFA study to provide insight into the structural requirements of ligand binding to the ileal bile acid transporter.

Experimental

Chemicals

3β-Hydroxy-5α-cholan-24-oic acid (**13**), methylcholate (**14**), ursocholate (**15**), 5β-cholanic acid (**16**), deoxycholate (**17**), chenodeoxycholate (**18**), and lithocholate (**19**) were purchased from Steraloids Inc. (Wilton, NH). Bile acid–peptide conjugates (**3**–**12**) were synthesized as described previously [16,17]. 3α,7α,12α-Triformyloxy-cholic acid (**22**), 3α-hydroxy-7α,12α-diformyloxy-cholic acid (**23**), and 3-oxo-7α,12α-dihydroxycholic acid (**21**) were synthesized according to the method of Kramer and Schneider [18]. 3α-Amino-7α,12α-dihydroxycholic acid (**20**) was synthesized according to Schneider et al. [19].

Cell culture and biological data

CaCo-2 cells were cultured as described previously [17]. Apical to basolateral transepithelial transport of [^{14}C]-taurocholic acid was studied in the presence or absence (control) of a 100-fold excess of a bile acid conjugate. Samples of 100 µl were taken from the basolateral side at designated times and replaced with fresh 100 µl transport solution. The amount of radiolabeled material in the samples was determined using a Beckman LS-5801 liquid scintillation counter. The transport rate was calculated by

linear regression from the amount recovered on the basolateral side during the experiment. Percent inhibition of transepithelial transport was calculated by comparing the apparent transport rate in the presence of an inhibitor against the control.

Molecular modeling, alignment rules and conformational search

Molecular models of the ligands were constructed using standard bond distances and bond angles with the molecular software package SYBYL v. 6.3 [20], mounted on a Silicon Graphics Iris Indigo workstation. The starting coordinates of the cholate and taurocholate derivatives were all taken from the crystallographic coordinates [21, 22]. However, the conformations of the taurocholic and cholic acid derivatives, as present in the Cambridge Structural Database (CSD), vary in one specific torsional angle (Ψ) in the C17 side chain (C17-C20-C22-C23). In cholic acid derivatives, Ψ is 69.3°, whereas the same torsional angle is 126° in taurocholic derivatives. The success of a CoMFA study is strongly influenced by the alignment of the various molecules in the analyzed set. In order to minimize the effect of badly aligned groups on the overall outcome of the CoMFA, we searched for a mutually equal alignment of the C17 side chains. Conformational searching of the side chains was performed by the GridSearch subroutine in SYBYL using a 360° perturbation of Ψ with an angle increment of 10°. The resulting conformations and calculated energies were stored in a molecular spreadsheet for analysis.

All bile acid conjugates in Table 1 were superposed on taurocholic acid using the carbon atoms 3, 7, 12, and 17 as templates for a rigid fit procedure. Side chains extending beyond C17, if present, were fitted on the lowest energy conformer of compound **11**. Structural refinement of the flexible peptide backbone in this compound was carried out using molecular dynamics simulations with a target temperature of 300 K, a step interval of 1.0 fs, and a heating cooling rate of 1.0 kcal/atom ps. After a 10 ps equilibration period, conformations were sampled, their energy calculated, and stored in a database every 500 fs for a total of 1.0 ns. During these runs, movement of the cholic acid backbone was restricted.

The compounds in this study were divided into a training set (25 compounds) and a test set (5 compounds). Since the database of bile acid derivatives comprises analogs with substitutions and derivatizations at the 3, 7, 12, and 17 positions, the candidates for the test set were randomly selected from these subgroups. The rigid structure of the cholestane backbone allows a good superpositioning of the test set.

Theoretical descriptors and computational methods

Point charges on all atoms of the molecules used in this study were calculated using the AM1 Hamiltonian within the MOPAC suite of programs [23]. Molecular mechanics corrections were made to any CO-NH bond (MMOK). Other keywords in these calculations included EF, NOINTER and PRECISE. The octanol/water partition coefficient (clogP) and molar refractivity index (CMR) were calculated using the Daylight software package [24].

'Classic' QSAR

To assess the correlation between clogP, CMR and carrier affinity, a QSAR was carried out by multiple linear regression using the multivariate general linear hypothesis (MGLH) module in the SYSTAT 5.1 [25] statistical software package. During these runs, biological data were fixed as dependent variables and clogP and CMR values were inferred as independent variables.

CoMFA: Interaction energies and regression techniques

CoMFA was carried out using the QSAR module in SYBYL. The steric and electrostatic field energies were calculated using an sp^3 carbon probe atom with a charge of +1 and a distance-dependent dielectric constant at all intersections of a regularly spaced (2.0 Å) grid. The dimensions of the CoMFA lattice were determined through an automatic procedure, featured by the SYBYL/CoMFA routine, which insures that the lattice walls extend beyond the dimension of each structure by 4.0 Å in all directions. Steric and electrostatic contributions were truncated to a value of ±30 kcal/mol, and the electrostatic contributions at lattice intersections yielding maximal steric values were ignored. All regression analyses were done using the partial least-squares (PLS) algorithms in SYBYL. Initial analyses were performed using full cross-validation (leave-one-out method). The analyses were performed with a scaling according to standard deviations (using the keyword CoMFA_STD). The optimal number of components to be used in the non-cross-validated analyses was defined as that yielding the highest cross-validated r^2 value (q^2). To minimize the influence of noisy columns, all cross-validated analyses were performed at a minimum σ (column filter) of 2.0 kcal/mol.

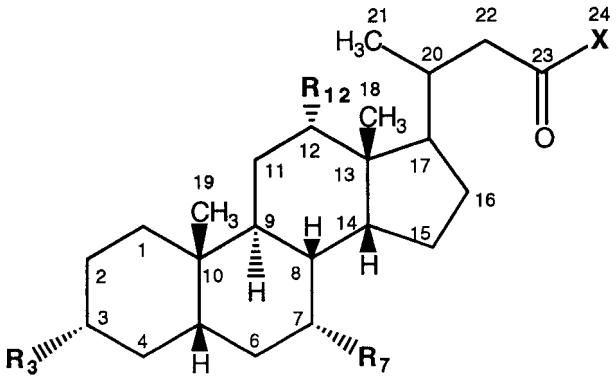

Fig. 1. General structural formula of bile acid analogs. The torsional angle Ψ is defined by C17-C20-C22-C23.

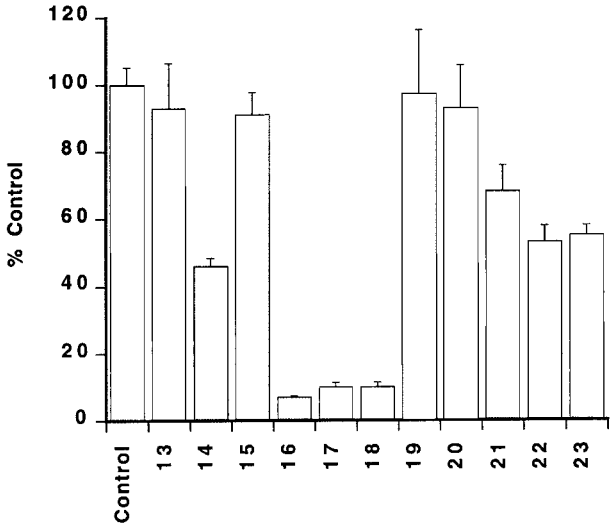

Fig. 2. Inhibition studies with bile acid analogs. The percent inhibition was calculated from the difference of [^{14}C]-taurocholic acid transport in the presence and absence (control) of bile acid derivatives. (See Table 1 and Fig. 1 for structures of the compounds.)

Results and Discussion

Biological data

The ability of bile acid conjugates (Fig. 1) to inhibit taurocholic acid transport in CaCo-2 cells (Fig. 2) varied from being undetectable for the monohydroxy bile acids **13**, **15**, and **19** to an almost complete inhibition by the dihydroxy bile acids **16**–**18** (Fig. 2). The zwitterionic bile acid **20** had no effect on transepithelial transport of [^{14}C]-taurocholic acid, suggesting that a positive charge around the C3 position abolishes affinity for the carrier. The methylester of cholic acid, **14**, shows decreased affinity for the carrier. However, the methylation of the C24 carboxylic acid group does not completely prevent interaction with the transporter, which is not in agreement with the generally accepted theory that a negatively charged moiety around the C24 position is essential for recognition by the intestinal bile acid transporter. This suggests that substrates with a free carboxylic acid group around the C24 position as well as substrates with an electron donor group (negative dipole) in this region are compatible with affinity for the bile acid transporter.

Even though no free hydroxyl groups are present, the formyl esters **22** and **23** inhibit [^{14}C]-taurocholic acid transport, albeit with decreased affinity compared to tri- and dihydroxy bile acids. The introduction of an oxo-group at position C3 (compound **21**) has a dramatic effect on carrier affinity, even though two free hydroxyl groups are present in the molecule.

Conformational search and structural alignment

Figure 3 shows the results of the GridSearch subroutine on the C17-C20-C22-C23 torsional angle Ψ in cholic acid and taurocholic acid. In comparing the two structures, a lower conformational energy (Tripos force field) well can be found between 50° and 70°. Accordingly, we modified the side chain of taurocholic acid and kept the torsional angle of the cholic acid side chain intact. The taurocholic torsion angle Ψ was subsequently set to 69.3°, which is identical to the same torsion angle in cholic acid.

The molecules were superimposed by overlaying the atoms with atom numbers 3, 7, 12, and 17 of the rigid cholestane backbone (data not shown).

Classic QSAR

Analysis of the correlation between carrier affinity of the data set and clogP and CMR was carried out by multilinear regression analysis. The variability in the biological activity parameter '1/%inhibition' was best explained by clogP or CMR alone with an adjusted multiple r^2 of 0.041 and 0.037, respectively. These results indicate a poor correlation between the theoretical descriptors CMR and logP and the measured affinity data and validate the use of a 3D QSAR.

CoMFA

The bile acid derivatives used in this CoMFA study are reported in Table 1. The compounds in this study were divided into a training set (25 compounds) and a test set (5 compounds). Since the database of bile acid derivatives comprises analogs with substitutions and derivatizations at the 3, 7, 12, and 17 positions, the candidates for the test set were randomly selected from these subgroups. The 3D QSAR of the training set was carried out by cross-validated PLS analyses on CMR, cLogP, steric and electrostatic CoMFA fields, and several different empirical

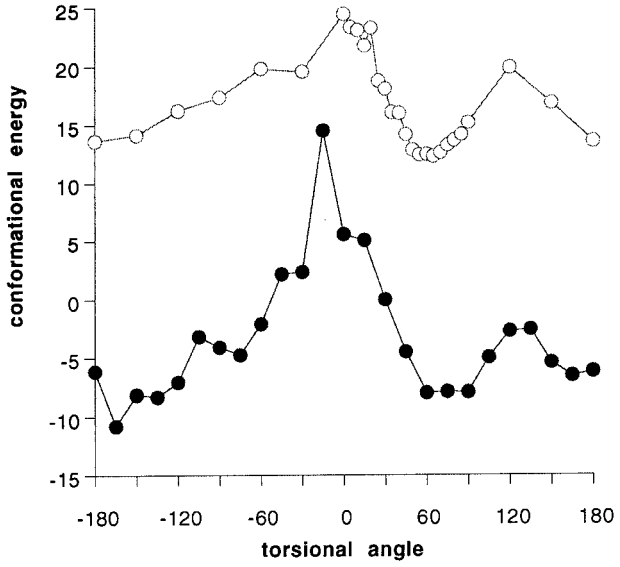

Fig. 3. GRID search plot of torsional angle Ψ in cholic acid (open circles, initial Ψ = 69.3°) and taurocholic acid (filled circles, initial Ψ = 126°). The conformational energy (Tripos force field) was calculated while rotating the torsional angle Ψ of these two compounds.

TABLE 2
RELATIVE CONTRIBUTIONS OF FINAL CoMFA TO THE BIOLOGICAL ACTIVITY (1/%inhibition)

Contribution	Normalization coefficient	Fraction
Steric	1.012	0.280
Electrostatic	2.598	0.720

and theoretical dependent variables, such as K_i, $1/K_i$, $\log K_i$, %inhibition, log(%inhibition), and 1/%inhibition. The relative contribution of the independent variables cLogP and CMR to the overall CoMFA model was low, generally accounting for less than 10% of the model variability (data not shown). Therefore, these descriptive parameters were excluded from further analysis.

The dropping of variables, based upon the standard deviation cutoff, allowed us to use only 411 potentially relevant columns in the CoMFA model out of a total of 3744 columns. The first analyses with K_i, %inhibition, log(%inhibition), and $\log K_i$ resulted in low q^2 values (data not shown). The reciprocal values of K_i and %inhibition gave a good correlation with the CoMFA field description. However, the K_i values for these compounds were mathematically derived from the inhibition data (using the Lineweaver–Burke expression for competitive inhibition with after correction for the passive transport component of taurocholic acid), which adds uncertainty to these values and will therefore increase variability in the resulting model. Because of this direct relationship between %inhibition and K_i and the – presumably – higher error in calculated K_i values, we decided to drop the latter as an independent variable for carrier affinity. The relative contributions of the CoMFA variables to the model are listed in Table 2. These values constitute useful information to better understand to what amount the various steric and electrostatic regions influence the binding to the transporter. The fact that the electrostatic contribution is significantly higher than the steric one (72% versus 28%, respectively) means that the 1/%inhibition values of substrates for the ileal bile acid transporter are highly dependent on the molecular charge of the ligand. The final model rationalizes the steric and electrostatic factors which modulate affinity to the bile acid carrier with a q^2 of 0.633. The conventional r^2 for this analysis was 0.958, using one principal component as suggested by the cross-validated PLS run. Furthermore, this model expressed good predictive capability for the test set of bile acid derivatives ($r^2_{pred} = 0.692$; Table 3).

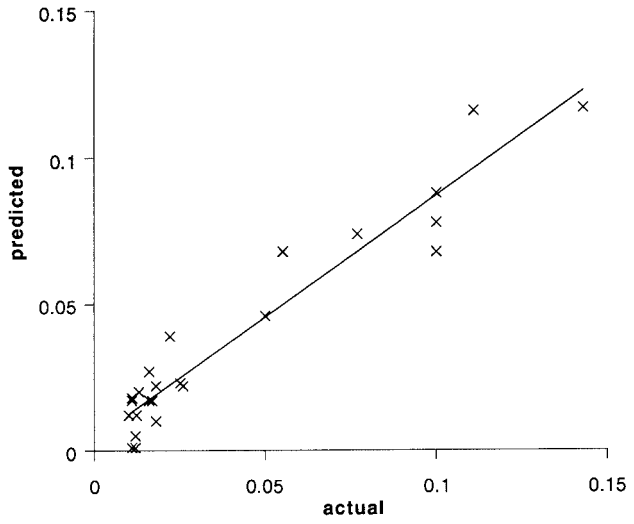

Fig. 4. Plot of observed versus predicted 1/%inhibition values according to CoMFA analysis.

TABLE 3
RESULTS OF THE 'TEST SET'

Compound #	1/%inhibition	
	Experimental	Predicted
8	0.015	0.0145
10	0.0168	0.0172
12	0.0138	0.0135
13	0.0108	0.0110
20	0.011	0.0096

The statistical results of the final CoMFA are represented in Fig. 4 as a plot of experimental and calculated values of 1/%inhibition. The line indicating the linear correlation between actual and predicted values has a slope of 0.831 and an intercept of 0.004.

CoMFA contour maps (Figs. 5 and 6) were generated by interpolating points in the CoMFA lattice with extremely high or low steric and electrostatic interaction energy. The field values were calculated as the scalar product of the β-coefficient and the standard deviation associated with a particular column in the QSAR table (stdev*coeff). The values corresponding to steric columns are plotted as the percentage of contribution to the QSAR relation. In Fig. 5, areas of high steric bulk tolerance (80% contribution) are represented by green polyhedra. The yellow contours describe regions of space where an increase in steric bulk leads to a decreased affinity for the bile acid transporter. It is interesting to note that a large yellow region surrounds the side where the hydroxyl groups are attached to the bile acids. It was previously shown that the number of hydroxyl groups has a large effect on the affinity for the bile acid carrier; substitution of these groups by larger moieties could lead to decreased affinity. It is unclear whether this is due to loss of hydrogen bonding interaction when the hydroxyl groups are removed or from steric hindrance by the introduction of steric bulk around these positions, thus preventing the molecule from interacting with the transporter.

The end of the C17 side chain shows a favorable region for the addition of steric bulk. Therefore, extension of the flexible side chain with apolar groups can increase the affinity of a ligand for the ileal bile acid carrier.

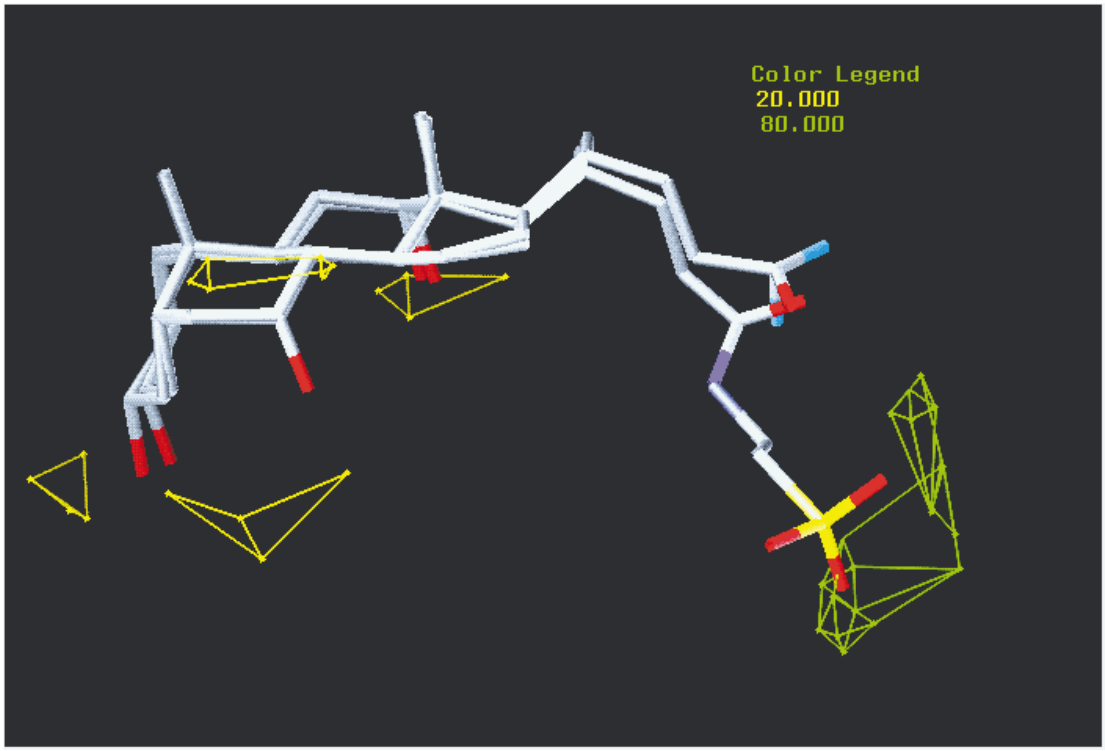

Fig. 5. The CoMFA steric stdev*coeff contour plot. Sterically favored areas (contribution level of 80%) are represented by green polyhedra. Sterically disfavored areas (contribution level of 20%) are represented by yellow polyhedra. Active molecules **1** (cholic acid) and **2** (taurocholic acid) are shown for reference.

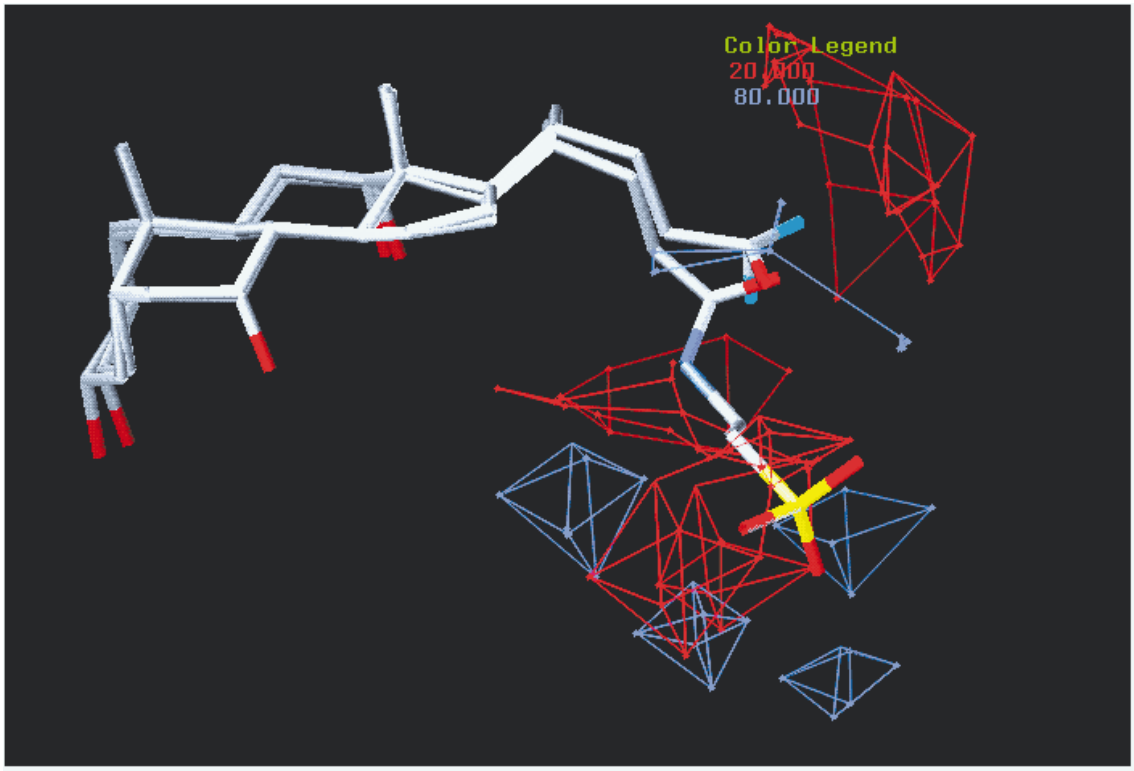

Fig. 6. The CoMFA electrostatic stdev*coeff contour plot. Negative charge favored areas (contribution level of 80%) are represented by red polyhedra. Positive charge favored areas (contribution level of 20%) are represented by blue polyhedra. Active molecules **1** (cholic acid) and **2** (taurocholic acid) are shown for reference. Blue and red regions indicate areas with low and high electron density, respectively.

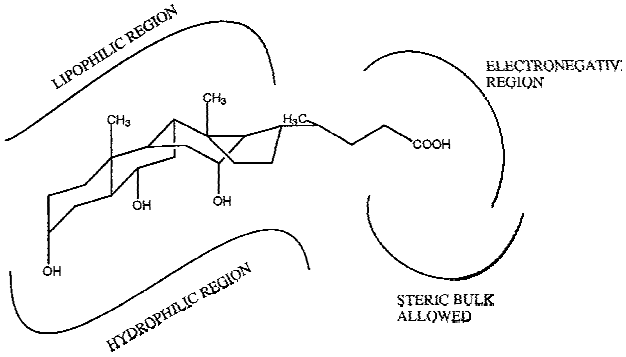

Fig. 7. Low-resolution model for substrate recognition by the ileal bile acid carrier.

The electrostatic contribution contour plot from the analysis is plotted as the stdev*coeff field in Fig. 6. The red polyhedra (80% contribution) indicate areas where high electron density increases affinity and are primarily located around the C24–C27 area in the vicinity of the free carboxylic acid and sulfate group in cholic acid analogs and taurocholic acid analogs, respectively. Groups with high electron density in these areas have been recognized previously to be necessary for interaction with the carrier [2]. This area probably plays an important role in electrostatic attraction of substrates by a positively charged site in the ileal bile acid carrier. Areas of decreased tolerance for negative charge (20% contribution), designated by blue polyhedra, are noted beyond the C27 position in taurocholic acid. This could indicate that the positioning of a group with high electron density is critical for interaction with the intestinal bile acid carrier. For maximal interaction, this group should be situated between C24 and C27.

Conclusions

Figure 7 is a low-resolution model for ligand binding to the ileal bile acid transporter which can serve as a guideline for drug design. There are a number of regions of the ligand that the model is silent on due to lack of structural variability at this specific place in the compounds used for the CoMFA study.

A large electronegative region is identified at the position where most substrates possess a negatively charged subunit, either a carboxylate or a sulfate moiety. Positive charge or neutral groups in this position diminish affinity for the transporter as illustrated by compounds **24** and **26**. Both compounds are lysyl derivatives possessing a positively charged amino side chain in this region. The position of the negative group is also of vital importance, leading to a dramatic decrease in affinity if the charged subunit is introduced far beyond position 24 in the cholestane backbone (e.g., compound **29**).

The introduction of steric bulk at the end of the side chain can have a positive effect on carrier affinity, which indicates that the bile acid carrier has flexibility towards substrates with altered C24 sequences.

The 3D orientation of the bile salt molecule shows a hydrophilic region where the three hydroxy groups are oriented in the same direction. The number of hydroxy groups in a ligand in this region is directly related to affinity, while steric bulk in this area is prohibited and decreases binding to the transporter. A lipophilic region is identified where the methyl moieties are opposite of the hydroxyl groups.

Summarizing, this study complements previous structure–affinity work on the ileal bile acid carrier and provides a low-resolution blueprint for the rational design and synthesis of bile acid conjugates that may improve the absorption of peptides or other drugs that are attached to a bile acid. Alternatively, it provides insight into the design of molecules that could inhibit intestinal bile acid absorption.

Acknowledgements

The authors express their thanks to Dr. Richard Guy for the use of his workstation and to Dr. Irwin D. Kuntz and the Computer Graphics Laboratory (NIH P41-RR01081) for their computing support. This work was supported in part by the Universitywide AIDS Research Program (UARP R93SF061 to S.Ø. and F95SF036 to P.W.S.) and an FIP Fellowship to P.W.S.

References

1 Johnson, L. (Ed.) Physiology of the Gastrointestinal Tract, 2nd ed., Raven Press, New York, NY, U.S.A., 1987, pp. 1557–1580.
2 Swaan, P.W., Szoka Jr., F.C. and Øie, S., Adv. Drug Deliv. Rev., 20 (1996) 59.
3 Kramer, W., Burckhardt, G., Wilson, F.A. and Kurz, G., J. Biol. Chem., 258 (1983) 3623.
4 Lin, M.C., Kramer, W. and Wilson, F.A., J. Biol. Chem., 265 (1990) 14986.
5 Lin, M.C., Weinberg, S.L., Kramer, W., Burckhardt, G. and Wilson, F.A., J. Membr. Biol., 106 (1988) 1.
6 Burckhardt, G., Kramer, W., Kurz, G. and Wilson, F.A., J. Biol. Chem., 258 (1983) 3618.
7 Schiff, E.R., Small, N.C. and Dietschy, J.M., J. Clin. Invest., 51 (1972) 1351.
8 Heaton, K.W. and Lack, L., Am. J. Physiol., 214 (1968) 585.
9 Kramer, W., Wess, G., Neckermann, G., Schubert, G., Fink, J., Girbig, F., Gutjahr, U., Kowalewski, S., Baringhaus, K.H. and Boger, G., J. Biol. Chem., 269 (1994) 10621.
10 Wess, G., Kramer, W., Enhsen, A., Glombik, H., Baringhaus, K.H., Boger, G., Urmann, M., Bock, K., Kleine, H., Neckermann, G., Hoffmann, A., Pittius, C., Falk, E., Fehlhaber, H.W., Kogler, H. and Friedrich, M., J. Med. Chem., 37 (1994) 873.
11 Cramer III, R.D., Patterson, D. and Bunce, J., J. Am. Chem. Soc., 110 (1988) 5959.
12 Recanatini, M., J. Comput.-Aided Mol. Design, 10 (1996) 74.

13 Tong, W., Collantes, E.R., Chen, Y. and Welsh, W.J., J. Med. Chem., 39 (1996) 380.
14 Siddiqi, S.M., Pearlstein, R.A., Sanders, L.H. and Jacobson, K.A., Bioorg. Med. Chem., 3 (1995) 1331.
15 Kubinyi, H. (Ed.) 3D QSAR in Drug Design: Theory, Methods and Applications, ESCOM, Leiden, The Netherlands, 1993.
16 Kågedahl, M., Swaan, P.W., Redemann, C.T., Tang, M., Craik, C.S., Szoka Jr., F.C. and Øie, S., Pharm. Res., 14 (1997) 176.
17 Swaan, P.W., Hillgren, K.M., Szoka Jr., F.C. and Øie, S., Bioconj. Chem., 8 (1997) 520.
18 Kramer, W. and Schneider, S., J. Lipid Res., 30 (1989) 1281.
19 Schneider, S., Schramm, U., Schreyer, A., Buscher, H.-P., Gerok, W. and Kurz, G., J. Lipid Res., 32 (1991) 1755.
20 SYBYL v. 6.3, Tripos Associates, St. Louis, MO, U.S.A.
21 Miki, K., Kasai, N., Shibakami, M., Chirachanchai, S., Takemoto, K. and Miyata, M., Acta Crystallogr., C46 (1990) 2442.
22 Campanelli, A.R., de Sanctis, S.C., D'Archivio, A.A., Giglio, E. and Scaramuzza, L., J. Incl. Phen., 11 (1991) 247.
23 MOPAC 6.0, Quantum Chemistry Exchange Program, No. 455.
24 Daylight software package, release 4.4, Daylight Chemical Information Systems Inc., Mission Viejo, CA, U.S.A.
25 SYSTAT, SPSS Inc. Chicago, IL, U.S.A.